

# Flexible Pressure Sensor With High Sensitivity and Low Hysteresis Based on a Hierarchically Microstructured Electrode

Wen Cheng, Jun Wang, Zhong Ma, Ke Yan, Yunmu Wang, Huiting Wang,  
Sheng Li, Yun Li, Lijia Pan<sup>✉</sup>, Member, IEEE, and Yi Shi

**Abstract**—Flexible pressure sensors are crucial for E-skins to enable tactile sensing capabilities. However, flexible pressure sensors often exhibit high hysteretic response caused by internal and external mechanical dissipations in flexible materials. The hysteresis gives rise to reliability issues, especially in the presence of dynamic stress. In this letter, we report a flexible capacitive pressure sensor design with hierarchically microstructured electrodes to obtain both high sensitivity and low hysteresis. The sparsely spaced large pyramid microstructure improves the sensitivity, whereas the small pyramid reduces the hysteresis caused by interfacial adhesion. The optimized sensor shows excellent performances in terms of high sensitivity ( $\sim 3.73 \text{ kPa}^{-1}$ ), ultralow detection limits (0.1 Pa), significantly reduced hysteresis ( $\sim 4.42\%$ ), and enhanced sensing capability for pluses, which demonstrates its potential for advanced electronic skins.

**Index Terms**—Pressure sensor, flexible, hysteresis, sensitivity.

## I. INTRODUCTION

ELECTRONIC skins show great potential for artificial intelligence applications, including wearable healthcare device, intelligent robots, and biomimetic prosthetics [1]–[12]. Pressure sensing is one of the most important functions of electronic skin [3]. In recent years, researchers sought methods to develop flexible pressure sensors with sensitivity that surpasses human skin, and most of them have tried to decrease the apparent Young's modulus by using soft materials and microstructures [10]–[15]. With a lower apparent Young's modulus, these flexible materials have a larger deformation, and hence, a higher sensitivity; however, the tradeoff is a high hysteresis resulted from internal and interfacial energy dissipation. For example, pressure

Manuscript received November 10, 2017; revised December 7, 2017, December 12, 2017, and December 13, 2017; accepted December 13, 2017. Date of publication December 18, 2017; date of current version January 25, 2018. This work was supported in part by the National Key Research and Development program of China under Grant 2017YFA0206301, in part by the National Natural Science Foundation of China under Grant 61674078 and Grant 1157436, in part by the Jiangsu Natural Science Foundation under Grant BK20130055, and in part by the PAPD program. The review of this letter was arranged by Editor M. Tabib-Azar. (*Corresponding author: Lijia Pan.*)

The authors are with the Collaborative Innovation Center of Advanced Microstructures, School of Electronic Science and Engineering, Nanjing University, Nanjing 210093, China (e-mail: lpan@nju.edu.cn).

Digital Object Identifier 10.1109/LED.2017.2784538

sensors with following materials show obvious hysteresis: Au nanowires coated tissue paper show a sensitivity of  $1.14 \text{ kPa}^{-1}$  and hysteresis of  $\sim 38\%$  [16], polypyrrole with a hollow-sphere microstructures show a sensitivity of  $133.1 \text{ kPa}^{-1}$  and hysteresis of  $\sim 35\%$  [17], a dielectric layer composed of micropyramidal rubber shows a sensitivity of  $0.55 \text{ kPa}^{-1}$  and hysteresis of  $\sim 11.5\%$  [18], carbon-based cellular elastomers show a sensitivity of  $10 \text{ kPa}^{-1}$  and hysteresis of  $\sim 45\%$  [19]. The hysteresis of pressure dependent electric properties leads to a large difference in the reading outputs between loading and unloading for the same pressure, especially in a dynamic loading-unloading process [8], [20]–[23].

In this letter, we report the design of flexible capacitive pressure sensors with both high sensitivity and low hysteresis by adopting a hierarchical pyramid microstructure design for the electrode. Inserting small pyramid arrays into large pyramid lattices reduces the hysteresis caused by interfacial adhesion, and decreasing the area density of large pyramids is favorable for better sensitivity. As a result, the sensor exhibited high sensitivity ( $3.73 \text{ kPa}^{-1}$ ), an ultralow detection limit (0.1 Pa), and a low hysteresis ( $\sim 4.42\%$ ), which allows precise measurement of wrist pulse. The results demonstrate the importance of reduced hysteresis of flexible pressure sensors for the application of electronic skins.

## II. EXPERIMENTAL DETAILS

### A. Microstructure Design and Fabrication

The microstructured polydimethylsiloxane (PDMS) films were replicated from molds of  $<100>$  Si wafer with 300 nm thermally grown oxide, which were patterned into inverted pyramid structure by using photolithography and anisotropically wet etching [24]. Octadecyltrichlorosilane (OTS) was vapor-deposited on the Si mold as a release agent. Then liquid PDMS (10:1, Sylgard 184) was cast onto the molds and cured at  $70^\circ\text{C}$  for 2 h. The sensors adopt a double-layered structure (Fig. 1). The top layer is a  $6\text{-}\mu\text{m}$ -thick biaxially oriented polypropylene (BOPP) film (from FSPG Hi-tech Co., LTD., sputtered with Pt on the top side), serving as the dielectric layer, and the bottom layer is a pyramid-microstructured PDMS film with a sputtered Pt layer ( $20 \sim 30 \text{ nm}$ ). We tested different electrode materials, including Pt, Au, and Al. We finally adopted Pt because Pt shows the best adhesion to

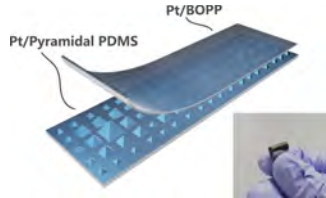


**Fig. 1.** Schematic illustration of the hierarchically structured pressure sensor, and an optical image of the sensor is shown in the inset.

the PDMS substrate; however, other metals are also viable options based on our device design.

### B. Characterizations and Pressure Sensing Test

The pressure sensors were characterized by an integrated system that consisted of a z-stage (Newmark), force gauge (Mark 10), and LCR meter (Agilent E4980). The pulse was tested with a sensor fixed on the arteries of the wrist, which was recorded using an impedance analyzer (Hioki IM3570).

### III. RESULTS AND DISCUSSION

For devices with single-sized pyramid microstructures, their sensitivity obviously trades off against hysteresis. Fig. 2(a) shows the scanning electron microscope (SEM) images of the pyramid microstructures corresponding to sensors with Microstructure 1 to Microstructure 8 (abbreviated as sensors M1 to M8), respectively. Note here ‘spacing’ is referred to as the distance between the tips of two neighboring pyramids. Fig. 2(c) plots the piezocapacitance of the sensors with pyramids of the same size but with different spacing in the range of  $0 \sim 100$  kPa. Both the sensitivity and hysteresis considerably increase as the pyramid spacing increases (lower density of pyramids in the same area). For example, sensor M1 (spacing of  $210 \mu\text{m}$ ) has a higher sensitivity of  $\sim 3.56 \text{ kPa}^{-1}$  but a larger hysteresis of  $18.2\%$ ; sensor M4 (spacing of  $35 \mu\text{m}$ ) has a lower sensitivity and lower hysteresis of  $\sim 0.510 \text{ kPa}^{-1}$  and  $6.44\%$ , respectively. With a lower density of pyramids, the microstructure has a lower apparent Young’s modulus, resulting in a larger piezocapacitance and higher sensitivity. However, this also resulted in a higher hysteresis, which is most likely caused by interfacial adhesion, as schematically illustrated in Fig. 2(b). The interfacial adhesion due to the van der Waals force between the pyramid-microstructured PDMS and the BOPP film can be expressed as:

$$G = kP^2L^2,$$

where  $G$  is the adhesive strength,  $P$  is the applied pressure,  $L$  is the spacing between adjacent pyramids, and  $k$  is a parameter related to the nature of the interface [22], [23], [25], [26]. This means that the interfacial hysteresis considerably increases when the spacing ( $L$ ) increases, which causes great uncertainty in the measurement of pressure. Another possible source of hysteresis, the viscoelastic hysteresis of PDMS, is small and can be ignored as calculated by the Bergstrom-Boyce model in Abaqus [6], [7].

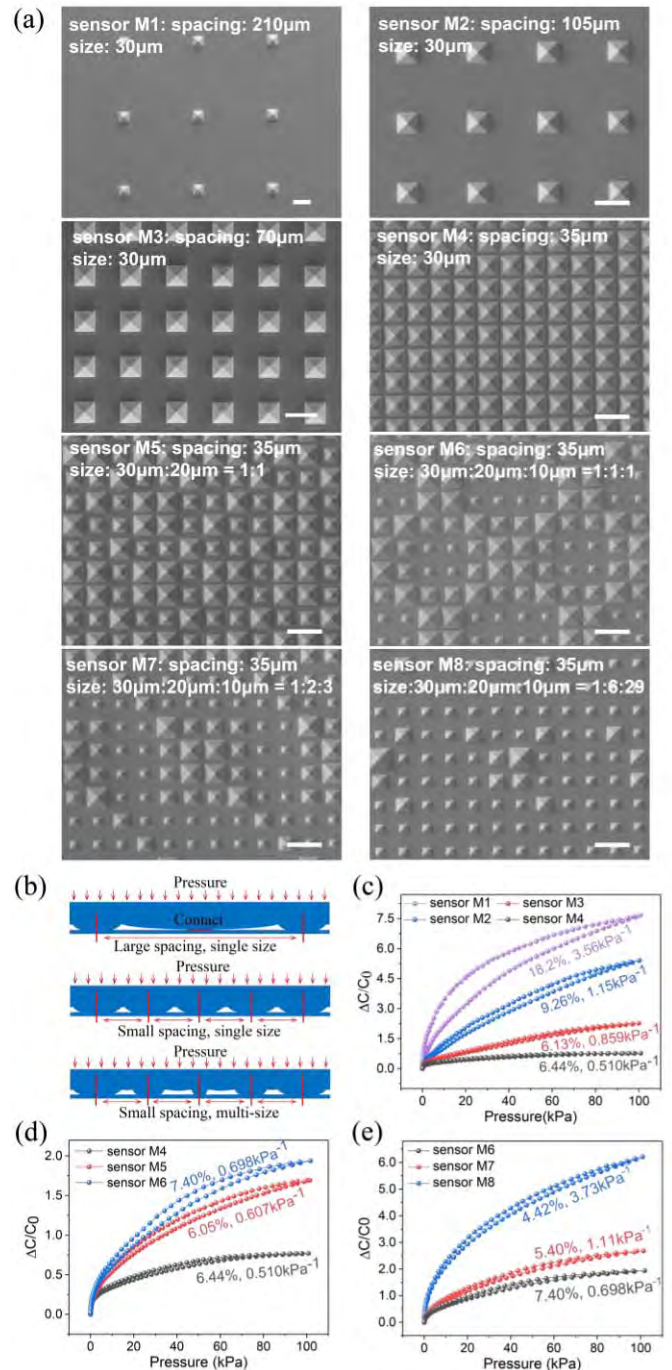


**Fig. 2.** Pressure sensors with hierarchical pyramids microstructures. (a) SEM images of the 8 differently designed pyramids microstructures for bottom electrodes of the pressure sensor, the inserted text denotes spacing and size of them. (b) Schematic illustration how hierarchical microstructures reduce interfacial adhesion of electrodes. Piezocapacitance of sensors with: (c) pyramids of the same size but different spacing; (d) pyramids of different sizes but the same spacing, (e) pyramids of multisize and the same spacing. Scale bar:  $50 \mu\text{m}$ .

The above analysis reveals that the spacing between adjacent pyramids is the key factor affecting both the sensitivity and hysteresis. We propose a hierarchically structured electrode that consists of pyramids with different sizes to increase the sensitivity and lower the interfacial adhesion. To quantitatively show the manipulation effect, the spacing

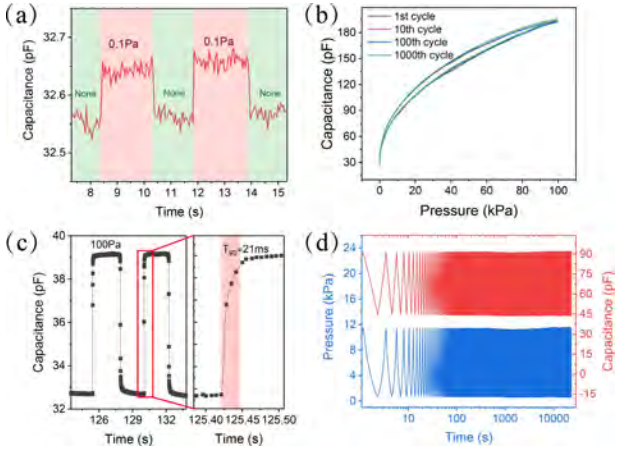


**Fig. 3.** Performance of the champion sensor (sensor M8). (a) Pressure detection limit test (0.1 Pa). (b) Selected cycles of the cyclic repeatability test. (c) T90 response time test ( $\sim 21\text{ms}$ ). (d) 10000 cycles of testing.

between the pyramids was set to a fixed value of  $35\text{ }\mu\text{m}$ , and the sizes and quantity ratio between different sized pyramids were regulated to tune the sensitivity and hysteresis. Fig. 2(d) shows the comparison of the M4-6 sensors consisting of electrodes with pyramids of  $30\text{ }\mu\text{m}$ ,  $30:20\text{ }\mu\text{m} = 1:1$ , and  $30:20:10\text{ }\mu\text{m} = 1:1:1$ , respectively. By using a multisized pyramidal microstructure, the device sensitivity increased from  $0.510\text{ kPa}^{-1}$  to  $0.698\text{ kPa}^{-1}$  due to the decreased density of the large pyramids of  $30\text{ }\mu\text{m}$ , and the hysteresis was controlled to be no larger than 7.40% due to the addition of small pyramids.

This strategy allowed us to further optimize the device performance. As shown as Fig. 2(e), by adopting a pyramid array of  $30:20:10\text{ }\mu\text{m} = 1:6:29$ , sensor M8 exhibited both a high sensitivity of  $3.73\text{ kPa}^{-1}$  (this value is among the highest ones for flexible capacitive pressure sensors [18], [27]–[29]), and a low hysteresis of 4.42%, beyond previous records [16], [17], [19], [29]–[31]. As presented in Fig. 3, sensor M8 shows excellent performances with an extremely low detection limit of 0.1 Pa, good repeatability, fast response ( $\sim 21\text{ ms}$ ), and excellent cycling stability (almost no decay over 10000 cycles).

Note our devices with relatively large capacitance allow simplified measurement by using BOPP as an ultrathin flexible dielectric film with very stable dielectric properties and a typical dielectric constant of 2.2. For sensor M8, the initial capacitance was  $\sim 27\text{ pF}$  at 0 kPa and the capacitance at 100 kPa was  $\sim 197\text{ pF}$ . In real-world applications, the noise fluctuations in the environment and circuits are often close to the pF level; our sensors have a high signal-to-noise ratio (SNR) and do not require sophisticated equipment for the measurement.

Furthermore, hierarchically structured sensors with low hysteresis are more favorable for accurate dynamic sensing, as exemplified by measuring, wrist pulses. Two highly sensitive pressure sensors, one with low hysteresis (sensor M8, hierarchical structure) and the other with high hysteresis (sensor M1, single type pyramids), were compared regarding the recorded wrist pulse waveforms. As presented in Fig. 4(a),

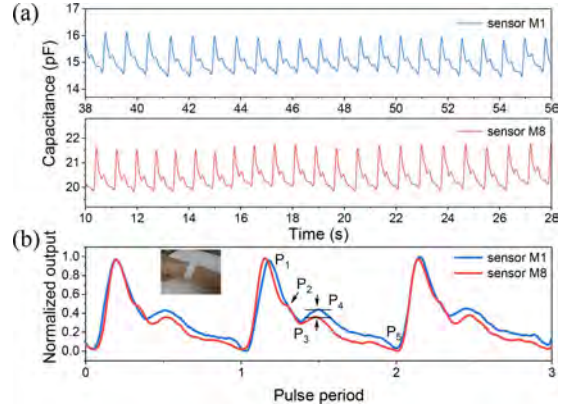


**Fig. 4.** An application of wrist pulse test using sensors with different hysteresis. (a) Pulse test using a high hysteresis sensor (sensor M1), and a low hysteresis sensor (sensor M8). (b) Comparison for the details of wrist pulse waveform detected by both sensors.

both sensors clearly and steadily recorded pulse waveforms due to the high sensitivity of both sensors; however, the enlarged pulse-period-normalized waveforms (Fig. 4(b)) shows the evident differences. Standard pulse waveforms should include a systolic peak ( $P_1$ ), a reflected systolic peak ( $P_2$ ), a dicrotic notch ( $P_3$ ), a diastolic peak ( $P_4$ ) and an end-diastolic notch ( $P_5$ ). However, sensor M1 lost the details of peak  $P_2$  between peaks  $P_1$  and  $P_2$ ; therefore, it is difficult to estimate the radial artery augmentation index (AI,  $\text{AI} = P_2/P_1$ ). Additionally, the reflectance index (RI,  $\text{RI} = P_4/P_1$ ) of sensor M1 was 38.9% higher than that of sensor M8 due to its large hysteresis. Therefore, sensors with low hysteresis are helpful to reduce the pulse waveform distortion and to accurately assess the stiffness of arteries for diagnosing hypertension, coronary atherosclerosis, and many other cardiovascular diseases [32]–[34]. All of these points indicate that hierarchically structured sensors with both a low hysteresis and high sensitivity are more suitable for precise dynamic sensing.

#### IV. CONCLUSION

We proposed a new design of pressure sensor using hierarchically micropyramid structures to significantly reduce hysteresis while maintaining its high sensitivity. The interfacial hysteresis is identified as an important factor for the large hysteresis of a flexible pressure sensor, which was rarely noticed in previous studies [13]. Due to the advantages of the hierarchical microstructure with reduced interfacial adhesion, we were able to generate a new device that exhibits a very low hysteresis of 4.42% and high sensitivity of  $3.73\text{ kPa}^{-1}$ . Our pulse sensing comparison showed that both features (the low hysteresis and high sensitivity) of the hierarchically microstructured device are essential to achieve accurate pulse information, which shows great potential for advanced electronic skin devices.

## REFERENCES

- [1] V. J. Lumelsky, M. S. Shur, and S. Wagner, "Sensitive skin," *IEEE Sensors J.*, vol. 1, no. 1, pp. 41–51, Jun. 2001, doi: [10.1109/JSEN.2001.923586](https://doi.org/10.1109/JSEN.2001.923586).
- [2] T. Someya, "Integration of organic field-effect transistors and rubbery pressure sensors for artificial skin applications," in *IEDM Tech. Dig.*, Washington, DC, USA, Dec. 2003, pp. 8.4.1–8.4.4.
- [3] M. L. Hammock, A. Chortos, B. C.-K. Tee, J. B.-H. Tok, and Z. Bao, "25th anniversary article: The evolution of electronic skin (E-Skin): A brief history, design considerations, and recent progress," *Adv. Mater.*, vol. 25, no. 42, pp. 5997–6038, Nov. 2013, doi: [10.1002/ADMA.201302240](https://doi.org/10.1002/ADMA.201302240).
- [4] X. Wang, L. Dong, H. Zhang, R. Yu, C. Pan, and Z. L. Wang, "Recent progress in electronic skin," *Adv. Sci.*, vol. 2, no. 10, pp. 1500169-1–1500169-21, Oct. 2015, doi: [10.1002/ADVS.201500169](https://doi.org/10.1002/ADVS.201500169).
- [5] R. S. Dahiya, G. Metta, M. Valle, and G. Sandini, "Tactile sensing—From humans to humanoids," *IEEE Trans. Robot.*, vol. 26, no. 1, pp. 1–20, Feb. 2010, doi: [10.1109/TRO.2009.2033627](https://doi.org/10.1109/TRO.2009.2033627).
- [6] A. Chortos, J. Liu, and Z. Bao, "Pursuing prosthetic electronic skin," *Nature Mater.*, vol. 15, no. 9, pp. 937–950, Jul. 2016, doi: [10.1038/NMAT4671](https://doi.org/10.1038/NMAT4671).
- [7] B. C.-K. Tee, A. Chortos, A. Berndt, A. K. Nguyen, A. Tom, A. McGuire, Z. C. Lin, K. Tien, W.-G. Bae, H. Wang, P. Mei, H.-H. Chou, B. Cui, K. Deisseroth, T. N. Ng, and Z. Bao, "A skin-inspired organic digital mechanoreceptor," *Science*, vol. 350, no. 6258, pp. 313–316, Oct. 2015, doi: [10.1126/SCIENCE.AAA9306](https://doi.org/10.1126/SCIENCE.AAA9306).
- [8] N. Luo, W. Dai, C. Li, Z. Zhou, L. Lu, C. C. Y. Poon, S.-C. Chen, Y. Zhang, and N. Zhao, "Flexible piezoresistive sensor patch enabling ultralow power cuffless blood pressure measurement," *Adv. Funct. Mater.*, vol. 26, no. 8, pp. 1178–1187, Feb. 2016, doi: [10.1002/ADFM.201504560](https://doi.org/10.1002/ADFM.201504560).
- [9] H. Li, Y. Xu, X. Li, Y. Chen, Y. Jiang, C. Zhang, B. Lu, J. Wang, Y. Ma, Y. Chen, Y. Huang, M. Ding, H. Su, G. Song, Y. Luo, and X. Feng, "Epidermal inorganic optoelectronics for blood oxygen measurement," *Adv. Healthcare Mater.*, vol. 6, no. 9, pp. 1601013-1–1601013-9, May 2017, doi: [10.1002/ADHM.201601013](https://doi.org/10.1002/ADHM.201601013).
- [10] B.-S. Park and T.-J. Ha, "Carbon-based pressure sensors with wavy configuration," *IEEE Electron Device Lett.*, vol. 38, no. 7, pp. 979–982, Jul. 2017, doi: [10.1109/LED.2017.2702614](https://doi.org/10.1109/LED.2017.2702614).
- [11] L. Wang, "Temperature interference reduction for pressure sensor made of conductive polymer composite," *IEEE Electron Device Lett.*, vol. 38, no. 1, pp. 123–125, Jan. 2017, doi: [10.1109/LED.2016.2625798](https://doi.org/10.1109/LED.2016.2625798).
- [12] D. J. Lipomi, M. Vosgueritchian, B. C.-K. Tee, S. L. Hellstrom, J. A. Lee, C. H. Fox, and Z. Bao, "Skin-like pressure and strain sensors based on transparent elastic films of carbon nanotubes," *Nature Nanotechnol.*, vol. 6, no. 12, pp. 788–792, Oct. 2011, doi: [10.1038/NNANO.2011.184](https://doi.org/10.1038/NNANO.2011.184).
- [13] M. Amjadi, K.-U. Kyung, I. Park, and M. Sitti, "Stretchable, skin-mountable, and wearable strain sensors and their potential applications: A review," *Adv. Funct. Mater.*, vol. 26, no. 11, pp. 1678–1698, Mar. 2016, doi: [10.1002/ADFM.201504755](https://doi.org/10.1002/ADFM.201504755).
- [14] M. I. Tiwana, S. J. Redmond, and N. H. Lovell, "A review of tactile sensing technologies with applications in biomedical engineering," *Sens. Actuators A, Phys.*, vol. 179, pp. 17–31, Jun. 2012, doi: [10.1016/J.SNA.2012.02.051](https://doi.org/10.1016/J.SNA.2012.02.051).
- [15] B. Zhuo, S. Chen, and X. Guo, "Micro structuring polydimethylsiloxane elastomer film with 3D printed mold for low cost and high sensitivity flexible capacitive pressure sensor," in *Proc. IEEE Electron Devices Technol. Manuf. Conf. (EDTM)*, Toyama, Japan, Feb./Mar. 2017, pp. 148–149.
- [16] S. Gong, W. Schwalb, Y. Wang, Y. Chen, Y. Tang, J. Si, B. Shirinzadeh, and W. Cheng, "A wearable and highly sensitive pressure sensor with ultrathin gold nanowires," *Nature Commun.*, vol. 5, Art. no. 3132, Feb. 2014, doi: [10.1038/NCOMMS4132](https://doi.org/10.1038/NCOMMS4132).
- [17] L. Pan, A. Chortos, G. Yu, Y. Wang, S. Isaacson, R. Allen, Y. Shi, R. Dauskardt, and Z. Bao, "An ultra-sensitive resistive pressure sensor based on hollow-sphere microstructure induced elasticity in conducting polymer film," *Nature Commun.*, vol. 5, Jan. 2014, Art. no. 3002, doi: [10.1038/NCOMMS4002](https://doi.org/10.1038/NCOMMS4002).
- [18] S. C. B. Mannsfeld, B. C.-K. Tee, R. M. Stoltzenberg, C. V. H.-H. Chen, S. Barman, B. V. O. Muir, A. N. Sokolov, C. Reese, and Z. Bao, "Highly sensitive flexible pressure sensors with microstructured rubber dielectric layers," *Nature Mater.*, vol. 9, no. 10, pp. 859–864, Oct. 2010, doi: [10.1038/NMAT2834](https://doi.org/10.1038/NMAT2834).
- [19] L. Qiu, M. B. Coskun, Y. Tang, J. Z. Liu, T. Alan, J. Ding, V.-T. Truong, and D. Li, "Ultrafast dynamic piezoresistive response of graphene-based cellular elastomers," *Adv. Mater.*, vol. 28, no. 1, pp. 194–200, Jan. 2016, doi: [10.1002/ADMA.201503957](https://doi.org/10.1002/ADMA.201503957).
- [20] J. S. Bergström and M. C. Boyce, "Constitutive modeling of the large strain time-dependent behavior of elastomers," *J. Mech. Phys. Solids*, vol. 46, no. 5, pp. 931–954, May 1998, doi: [10.1016/S0022-5096\(97\)00075-6](https://doi.org/10.1016/S0022-5096(97)00075-6).
- [21] J. S. Bergström and M. C. Boyce, "Constitutive modeling of the time-dependent and cyclic loading of elastomers and application to soft biological tissues," *Mech. Mater.*, vol. 33, no. 9, pp. 523–530, Sep. 2001, doi: [10.1016/S0167-6636\(01\)00070-9](https://doi.org/10.1016/S0167-6636(01)00070-9).
- [22] A. N. Gent and S.-M Lai, "Interfacial bonding, energy dissipation, and adhesion," *J. Polym. Sci. B, Polym. Phys.*, vol. 32, no. 8, pp. 1543–1555, Jun. 1994, doi: [10.1002/POLB.1994.090320826](https://doi.org/10.1002/POLB.1994.090320826).
- [23] K. L. Johnson, "Mechanics of adhesion," *Tribol. Int.*, vol. 31, no. 8, pp. 413–418, Aug. 1998, doi: [10.1007/978-0-387-92897-5\\_100873](https://doi.org/10.1007/978-0-387-92897-5_100873).
- [24] J. You, D. Kim, J. Y. Huh, H. J. Park, J. J. Pak, and C. S. Kang, "Experiments on anisotropic etching of Si in TMAH," *Sol. Energy Mater. Solar Cells*, vol. 66, nos. 1–4, pp. 37–44, Feb. 2001, doi: [10.1016/S0927-0248\(00\)00156-2](https://doi.org/10.1016/S0927-0248(00)00156-2).
- [25] K. R. Shull, "Contact mechanics and the adhesion of soft solids," *Mater. Sci. Eng., R, Rep.*, vol. 36, no. 1, pp. 1–45, Jan. 2002, doi: [10.1016/S0927-796X\(01\)00039-0](https://doi.org/10.1016/S0927-796X(01)00039-0).
- [26] F. W. DelRio, M. P. de Boer, J. A. Knapp, E. D. Reedy, Jr., P. J. Clews, and M. L. Dunn, "The role of van der Waals forces in adhesion of micromachined surfaces," *Nature Mater.*, vol. 4, no. 8, pp. 629–634, 2005, doi: [10.1038/NMAT1431](https://doi.org/10.1038/NMAT1431).
- [27] J. Lee, H. Kwon, J. Seo, S. Shin, J. H. Koo, C. Pang, S. Son, J. H. Kim, Y. H. Jang, D. E. Kim, and T. Lee, "Conductive fiber-based ultrasensitive textile pressure sensor for wearable electronics," *Adv. Mater.*, vol. 27, no. 15, pp. 2433–2439, Apr. 2015, doi: [10.1002/ADMA.201500009](https://doi.org/10.1002/ADMA.201500009).
- [28] J.-Y. Sun, C. Keplinger, G. M. Whitesides, and Z. Suo, "Ionic skin," *Adv. Mater.*, vol. 26, no. 45, pp. 7608–7614, Dec. 2014, doi: [10.1002/ADMA.201403441](https://doi.org/10.1002/ADMA.201403441).
- [29] Y. Kim, S. Jang, B. J. Kang, and J. H. Oh, "Fabrication of highly sensitive capacitive pressure sensors with electrospun polymer nanofibers," *Appl. Phys. Lett.*, vol. 111, no. 7, pp. 073502-1–073502-4, Aug. 2017, doi: [10.1063/1.4998465](https://doi.org/10.1063/1.4998465).
- [30] C. Pang, G.-Y. Lee, T.-I. Kim, S. M. Kim, H. N. Kim, S.-H. Ahn, and K.-Y. Suh, "A flexible and highly sensitive strain-gauge sensor using reversible interlocking of nanofibres," *Nature Mater.*, vol. 11, no. 9, pp. 795–801, Jul. 2012, doi: [10.1038/NMAT3380](https://doi.org/10.1038/NMAT3380).
- [31] L.-Q. Tao, K.-N. Zhang, H. Tian, Y. Liu, D.-Y. Wang, Y.-Q. Chen, Y. Yang, and T.-L. Ren, "Graphene-paper pressure sensor for detecting human motions," *ACS Nano*, vol. 11, no. 9, pp. 8790–8795, Sep. 2017, doi: [10.1021/ACSNANO.7B02826](https://doi.org/10.1021/ACSNANO.7B02826).
- [32] C. Dagdeviren, Y. Su, P. Joe, R. Yona, Y. Liu, Y.-S. Kim, Y. Huang, A. R. Damadoran, J. Xia, L. W. Martin, Y. Huang, and J. A. Rogers, "Conformable amplified lead zirconate titanate sensors with enhanced piezoelectric response for cutaneous pressure monitoring," *Nature Commun.*, vol. 5, Aug. 2014, Art. no. 4496, doi: [10.1038/NCOMMS5496](https://doi.org/10.1038/NCOMMS5496).
- [33] C.-H. Chen, C.-T. Ting, A. Nussbacher, E. Nevo, D. A. Kass, P. Pak, S.-P. Wang, M.-S. Chang, and F. C. P. Yin, "Validation of carotid artery tonometry as a means of estimating augmentation index of ascending aortic pressure," *Hypertension*, vol. 27, no. 2, pp. 168–175, Feb. 1996, doi: [10.1161/01.HYP.27.2.168](https://doi.org/10.1161/01.HYP.27.2.168).
- [34] S. Wällberg-Jonsson, K. Caidahl, N. Klintland, G. Nyberg, and S. Rantanpää-Dahlqvist, "Increased arterial stiffness and indication of endothelial dysfunction in long-standing rheumatoid arthritis," *Scandin. J. Rheumatol.*, vol. 37, pp. 1–5, Jul. 2009, doi: [10.1080/03009740701633238](https://doi.org/10.1080/03009740701633238).